Population Kinetics of a Repetitively-Pulsed Nanosecond Discharge

by

Benjamin T. Yee

A dissertation submitted in partial fulfillment
of the requirements for the degree of
Doctor of Philosophy
(Nuclear Engineering & Radiological Sciences)
in the University of Michigan
2013

Doctoral Committee:

Associate Professor John E. Foster, Chair
Doctor Edward V. Barnat, Sandia National Laboratories
Doctor Isaiah M. Blankson, National Aeronautics and Space Administration
Professor Augustus Evrard
Professor Mark J. Kushner

2013

I would like to dedicate this dissertation to someone else.

A C K N O W L E D G M E N T S

Who is this?

Preface

This is a dissertation about something; I really hope it's good.

TABLE OF CONTENTS

LIST OF FIGURES

LIST OF TABLES

LIST OF APPENDICES

LIST OF ABBREVIATIONS

RPND repetitively-pulsed nanosecond discharge

APP atmospheric-pressure plasma

VFP Vlasov-Fokker-Planck

EEDF electron energy distribution function

CHAPTER 1

Introduction

1.1 Overview

Historically, the study of atmospheric-pressure plasmas (APP's) is indistinguishable from the study of plasmas as a whole. However, the detail of the measurements and calculations associated with APP's has been limited by their complexity. From a computational perspective, the high pressure and number of potential reactions present a difficult challenge. Likewise, the high pressure can significantly complicate the data analysis for a number of plasma diagnostics. Aside from the high pressures, the large electric fields, short time scales, and general randomness of APP's make even the most basic observations a feat.

In the last several decades, some of this has begun to change. High-powered computing has allowed simulations with remarkable detail. Similarly, advances in technology has enabled plasma diagnostics in regimes that were experimentally inaccessible. As a result, the body of knowledge regarding APP's has greatly increased. Sometimes, the motivation for this work is scientific curiosity. More often, the study of APP's has been driven by a broad range of applications.

Among the first plasma applications were provided by APP's: ozone generation and lighting. Aside from these items, plasma welding, polymer treatment, combustion, and plasma televisions have become widely accepted. Meanwhile, a large number of new applications may soon be added to this list, including: treatment of tissue wounds, altering airflow over airfoils, and destruction of industrial pollutants.

Unsurprisingly, each case demands a different kind of plasma. The original arc discharges were created between two graphite rods connected to immense battery banks. In contrast, a modern research reactor studying plasma-assisted combustion might use a fast-switching semiconductor circuit. Over the years, several types of APPs have been developed for a variety of situations: dielectric-barrier, corona, thermal arc, RF, microwave, pulsed, and more.

Within this group[1], the repetitively-pulsed nanosecond discharge (RPND) has created considerable interest. Generally speaking, a RPND is a plasma generated by a repetitive electrical pulse applied between two electrodes. The pulse voltage is often in excess of one kilovolt, lasts anywhere from $< 1 - 100$ ns, and is repeated over a thousand times each second. The result is a wave of ionization (and light) which crosses from the powered electrode to the grounded one.

A RPND can fill volumes of several liters with a relatively uniform plasma. Though they can cause significant excitation of the background gas, they generally produce very little heating (in some cases below a detection limit of $\Delta \pm 15$ K). In addition, the excitation can be changed with adjustments to the magnitude or duration of the electrical pulse. Each of these characteristics are highly desirable in one or more of potential applications for APP's.

Given all of these promising properties, RPND's have been the subject of substantial study by several research groups. However, much of this work has focused on the physics of RPND's in air. Unfortunately, air's large number of constituent elements can lead to notable complexity. In turn, this can obscure some of the more fundamental questions relation to RPND's: how do they form, how is the energy distributed between excited particles, and what kind of spatial variation can be expected?

This paper details a study of each of these questions in a helium RPND. Specifically, the densities of one particular excited atom are measured for a variety of pressures and locations. This is complemented by measurements of the light emissions for the same set of parameters. A simple model of a RPND is used to predict several characteristics of the plasma based on the excited state densities: electron density, electric field, and light emission. The measured light emissions are interpreted to show how the energy is distributed in the gas, and how it changes over time. Finally, they are compared with the estimated light emissions to check the validity of several common assumptions.

The remainder of this chapter is comprised of a review of the associated literature, as well as a discussion of basic discharge theory. Chapter 3 covers the experimental setup as well as some general observations of the RPND. Next, the measurement of the excited state densities is presented, followed by the chapter on the light emission measurements. Chapter 6 explores the global model used to interpret the excited state densities, as well as some supporting particle-in-cell simulations. Finally, the paper concludes with a discussion of how the models and measurements impact the present understanding of RPND's.

[1]The interested reader is referred to Starikovskaia's review [1] which provides a general overview of APP's in the context of plasma-assisted combustion

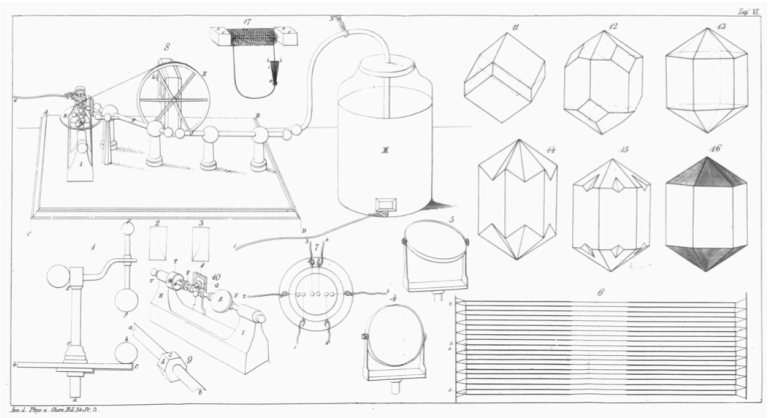

Figure 1.1: The experimental sketches of Wheatstone showing a traditional spark gap connected to a Leyden jar and electrostatic generator.

1.2 Literature Review

Though RPND's are very much a product of twentieth century research, they are fundamentally similar to a number of other pulsed discharges such as electrical sparks and lightning. Though Loeb united these disparate fields under the title of "ionizing waves of potential gradient" in 1964 [2] (we use the more familiar term, fast ionization waves), the underlying subjects had been under study since the Greeks who generated sparks by rubbing together amber and fur.

Despite these early observations, it was Leibniz in 1671 who first came to the conclusion that sparks were an electrical phenomena [3]. Subsequently, Franklin's famous kite experiment led him to a similar conclusion on the nature of lightning. Franklin was also involved in explaining the principles of Leyden jars, develop by Musschenbroek. The Leyden jar was the first reliable way to store electrical energy and proved a boon to later research.

In 1835, Wheatstone made the first attempt to measure the speed of electricity through a gas [4]. In his work, Wheatstone used a Leyden jar connected to two metal spheres, separated by a small gap. Once the charge in the jar reached a critical level, a spark would form in the gap. Figure 1.1 shows the experimental sketch provided by Wheatstone. Though the measurement is notable for its early date, it was later revisted with much more accuracy by Thomson [5]. Perhaps the most important outcome of Wheatstone's study was the observation by Zahn [6] that the speed of the light was *not* accompanied by a similar motion of the emitting particles.

Thomson's work concerned both the speed and direction of light in a pulsed discharge. Unlike Wheatstone's study, Thomson used an elongated tube, 15 m in length, and 5 mm in diameter, upon which he drew a vacuum. The original sketch of Thomson's discharge

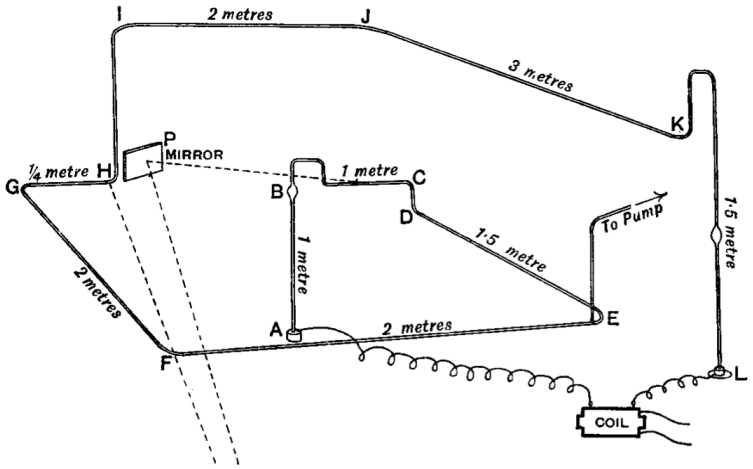

Figure 1.2: A sketch of J.J. Thomson's early experiments on fast ionization waves in long vacuum tubes.

apparatus can be seen in figure 1.2. Through a clever arrangement of mirrors, Thomson determined that the electricity had a speed approaching 1×10^{10} cm/s, and travelled from the anode to the cathode.

It was later, in 1930, that Beams would determine that the wave always initiated at the high voltage electrode, regardless of polarity [7]. In addition, Beams measured the current at the low potential electrode. He detected a current pulse which did not appear until after the light had completely crossed the gap. He came to the conclusion that the luminous front was likely the result of a moving region of ionization.

Around the same time, there was a distinct set of researchers ho were studying similar phenomena in lightning. In most cases, these studies concentrated on time-resolved photography, pioneered by Boys[2][8], and refined by Schonland [9]. This technique was later adopted by Allibone and Meek [10] to observe the evolution of a laboratory-generated spark.

By 1935, fast ionization waves had been under study for nearly 50 years. However, there was still no adequate explanation for the speed of the discharge. Similarly, Beams' observation that the wave always travelled from the high voltage to the low voltage electrode (regardless of polarity) was inconsistent with the Townsend model used to explain most plasmas. Based on observations made with fast pulses, Flegler and Raether developed a new theory of breakdown for sparks in air [11] which was capable of, at least partly, explaining the fast ionization wave phenomena. Independently, Loeb and Meek developed a similar theory in 1940 [12].

[2]In the same article, Boys anticipated a number of other atmospheric physics studies by proposing that rockets be fired at thunderclouds. Unfortunately, he lived in a village of thatched houses and could not conduct the experiment for fear of fire.

The work of Fleger and Raether as well as Loeb and Meek, was intended to explain the breakdown processes for an undetermined range of overvoltages (in excess of the breakdown voltage). However, as early as 1951, Fisher and Bederson [13], demonstrated that the Townsend mechanism was still plausible at low overvoltages.

In contrast, 1961 saw Fowler [14] seeking a hydrodynamic explanation for the waves. Contrary to the stochastic and particle-based description of the streamer breakdown, Fowler considered the luminous fronts to be nonlinear electron acoustic waves. Though the explanation provided a fair agreement with his observations, there were several issues with the analysis, namely a simplified consideration of the geometry and associated field strengths.

By 1965, Loeb himself, admits that photoionization was not insufficient on its own to produce the observed phenomena. In his review for Nature, Loeb identified several phenomena that exhibited similar characteristics. The return stroke in lighting, high overvoltage breakdown in rarefied gases, and sparks in atmosphere. Loeb was able to provide a qualitative description of the physics involved, but ultimately deferred on any quanitative description.

The insufficiency of photionization was later reinforced by the observation of Mesyats [15] that the speed of the discharge processes was often faster than the lifetimes of excited states. Again, this precluded photoionization from providing a significant amount of preionization for the propagation of an rpnd. Mesyats instead suggested that the large fields generated an electron avalanche that grew much more rapidly than the typical Townsend discharge. This was followed by an avalanche chain which further propagated the plasma.

Later, Kunhardt [16] extended on Mesyats' analysis and provided a more theoretical underpinning for it. Taking his inspiration from the group theory used in neutron diffusion, Kunhardt explored the development of a fiw from the perspective of "trapped" and "runaway" electrons. Previous work by Babich and Stankevich [**?**] inspired this by suggesting the existence of continually-accelerated electrons at high overvoltages.

As an aside, the topic of electron beams in rare gases became of substantial interest to researchers in the mid 1970s. Because rare gases lacked low-lying excited states which might detrimentally absorb energy, they were favor for laser where a population inversion could be achieved with ease. As a result, a great deal of work went into detailing the propagation of an electron beam in rare gases which is physically similar to the development of a fast ionization wave. However the primary difference between

It was around this time that the topic of fiw became of substantial interest to Russian research groups. Though much of the early work is shrouded in the mists of language differences, it is believed that Vasilyak [17] provides a fair review of the material.

Come 1998, the fiw was the subject of renewed interest by a group of researchers at the

Moscow Institute of Physics and Technology [18]. They employed several different diagnostic techniques (photomultiplier tubes and capacitive probes) in an exceptionally detailed study of fiws in both air and nitrogen, using a shock tube and a bell jar. A summary of these investigations can be found in [19]. The work showed exceptionally reproducibility of the discharge parameters at relatively low repetition rates, on the order of tens of Hz, and evidence of runaway electrons in the electronically excited molecular states. This work also included some of the first approximations of the electron energy distribution function (EEDF). This was found by comparing several paremeterized distribution functions with the resulting excited state populations.

This was time the population kinetics of an fiw was really examined. In this case, it emphasized the short-lived states of nitrogen. Specifically, [20] initially used the fiw to examine the population of electronic states of nitrogen. Later analysis [21] concluded that the, for a negative fiw in nitrogen, the vast majority of the electrons were generated in the aftermath of the wave and that the ionization did not track the luminous front. Additionally, measurements of the conductivity suggested that the local approximation becomes invalid in the wave front and the electron energy distribution function resembles a beam.

The development of fid semiconductor technology in the late 1990's and their commercialization in the early 2000's allowed the use of rpnds. Fundamentally, these discharges were the same as the fiws that had been studied for decades earlier. However, the much greater repetition rates (on the order of tens of kHz), meant that the discharges could be used in a number of previously impossible applications. Attention quickly turned toward plasma-assisted combustion [**?**], mhd energy bypass [22], and later, plasma actuators [23]. Additionaly studies, related to the development of high-pressure xenon lamps, led to several more quantitative models of the fiw development [24, 25]. These works also contributed to a semi-analytical energy coupling model as well [23].

Research efforts continued to use many of the same diagnostics as before. The current and voltage at the powered electrode were recorded (with varying levels of diligence), electric fields were measured with capacitive probes, and photomoultiplier tubes were used to measure the progress of the luminous front. The 2000's did add a few new tools to the diagnostic arsenal. Perhaps the most common addition is the use of ICCD's in order to record transition and broadband light. This approach has been used to verify the reproducibility of the discharge [23]. Though the gate times are still too short to capture the development of the wave, excitation profiles like those initially demonstrated by Vasilyak[17] are commonly recorded. Another, more exotic addition, has been the use of CARS. This nonlinear technique has proven to be excellent at reproducing the spatial temperature profiles of pulsed nanosecond discharges. This has become particularly interesting for groups interested in

applications to fast gas heating [26]. Others have used CARS to explore the electric field development of rpnds [**?**, **?**]. Finally, another research group has used LCIF to detect the radial and axial profiles of the metastable and electron densities in a helium discharge. The CARS and LCIF approaches are both notable for being active diagnostics of direct properties. This allows unprecedented time resolution and detail.

CHAPTER 2

Theory

2.1 Plasmas

A volume containing some number of charged particles can be considered a plasma if it meets three conditions. The first requires that the motion of charged particles is primarily determined by the electric and magnetic fields of the volume rather than through collisions with neutral particles. This is classically expressed by the inequality

$$\sqrt{n_{\mathrm{e}} e^2/(\varepsilon_0 m_{\mathrm{e}})} < \nu, \tag{2.1}$$

where n_{e} is the electron density, e is the fundamental charge, ε_0 is the permittivity of free space, m_{e} is the mass of an electron, and ν is the electron-neutral collision frequency. The left-hand side term is called the electron plasma frequency, it the characteristic frequency at which a plasma oscillates in response to a perturbation.

For a sufficiently large number of particles, the behavior of the each species of the plasma can be described by a continuous probability distribution function. This function, $f_\alpha(\vec{r}, \vec{v}, t)$, describes the probability of finding a particle of species α, at position $\vec{r}$, The distribution function for a particle can be determined by the Vlasov-Fokker-Planck VFP equation,

$$\frac{\partial f_\alpha}{\partial t} + \vec{v_\alpha} \cdot \nabla f_\alpha + q_\alpha \left(\vec{E} + \vec{v_\alpha} \times \vec{B} \right) \cdot \nabla_{\mathrm{v}} f_\alpha = \left(\frac{\partial f_\alpha}{\partial t} \right)_{\mathrm{coll}}. \tag{2.2}$$

Here, $\vec{E}$ is the electric field, $\vec{B}$ is the magnetic field, and $\partial f_\alpha/(\partial t)_{\mathrm{coll}}$ is a term representing all collisions. The VFP equation is coupled to Maxwell's equations in order to obtain a self-consistent description of the particle distribution and the resulting fields. In essence, this is the Boltzmann equation from statistical mechanics, however it now includes several changes. Vlasov replaced the original force term with the Lorentz equation, and Fokker and Planck introduced the collision operator on the right-hand side. This is coupled with

Maxwell's equations for a solution of the electric and magnetic fields in the plasma.

In the absence of external fields and with only elastic collisions, the equation admits the famous Maxwell-Boltzmann equilibrium distribution,

$$f_\alpha(v) = n\left(\frac{m_\alpha}{2\pi k_\mathrm{B}T}\right)^{3/2}\exp\left(-\frac{m_\alpha v_\alpha^2}{2k_\mathrm{B}T}\right), \tag{2.3}$$

where n is the number of degrees of freedom, k_B is Boltzmann's constant, and T is the temperature. A species of particles which possesses a Boltzmann distribution is said to be in equilibrium. Likewise, two species with the same distribution are in equilibrium.

Aside from this, the VFP equation is notoriously difficult to solve. As a result, most plasma models use various moments of equation 2.2 where the velocity dependence has been integrated out. These moments are the basis for the two-fluid equations, the MHD formulation, and global models. We will show the first three moments following the notation of Lieberman and Lichtenberg [27]. For example, the first moment is the continuity equation,

$$\frac{\partial n_\alpha}{\partial t} + \nabla\cdot(n_\alpha\vec{u_\alpha}) = G_\alpha - L_\alpha, \tag{2.4}$$

where $\vec{u_\alpha}$ is the mean velocity of species α, G_α is its rate of gain, and L_α is the rate of loss. This equation can be interpreted as the rate of change in particle density for a particular volume of space.

Though the continuity equation is much simpler than the original VFP equation, it cannot be solved alone. The mean velocity, $\vec{u}$, is undefined. Typically, this leads to the second moment,

$$mn_\alpha\left[\frac{\partial\vec{u_\alpha}}{\partial t}(\vec{u_\alpha}\cdot\nabla)\right] = q_\alpha n_\alpha(\vec{E}+\vec{u_\alpha}\times\vec{B}) - \nabla\cdot\vec{\Pi}_\alpha + \vec{f}_{\alpha,\mathrm{coll}} \tag{2.5}$$

where $\vec{\Pi}_\alpha$ is the pressure tensor, and $\vec{f}_{\alpha,c}$ is the rate of momentum transfer into species α. Again, any solution is stymied by the presence of a new a term, in this case, $\vec{\Pi}_\alpha$. At this point, an equation of state can be used to close the set of equations, in this case relating the pressure to the density. However, later work will benefit from one more moment.

Following the conservation of momentum, the energy conservation equation can be derived from the VFP equation,

$$\frac{\partial}{\partial t}\left(\frac{3}{2}p_\alpha\right) + \nabla\cdot\frac{3}{2}(p_\alpha\vec{u}_\alpha) + p_\alpha\nabla\cdot\vec{u}_\alpha + \nabla\cdot\vec{q}_\alpha = \frac{\partial}{\partial t}\left(\frac{3}{2}p_\alpha\right)\Bigg|_{\mathrm{coll}} \tag{2.6}$$

where p_α is the species pressure, q_α is the heat flow vector, and the right-hand side is the time rate of change in energy as a result of collisions. In our case, we only consider the flux

into the volume (from the electric field) and the distribution of this field via rate constants. This is the basis for the global model.

2.2 Atomic Spectroscopy

Spectroscopy spans a large body of theory which cannot be adequately covered here. Given that the measurements are all for helium, we will limit ourselves to a simple description of atomic spectroscopy. An atom is made of positively charged nucleus and a number of negatively charged electrons which orbit this nucleus. In the unperturbed, or ground state, the electrons occupy orbitals determined by a full solution of the Schrodinger equation.

However, interactions with other particles or photons can excite one or more of the electrons into orbitals with higher potential energy. In most cases relevant to low temperature plasmas, only a single electron will be excited at any given time. Depending on which orbital the electron is excited to, it can transition to orbitals with lower potential energy by emitting a photon. These are typically called allowed transitions.

Each orbital in an atom can be described by four quantum numbers.

- n - The principal quantum number.
- l - Orbital angular momentum number.
- j - Total angular momentum.
- m_j - Total angular magnetic moment.

The Pauli exclusion principle restricts more than a single electron from occupying any given state defined by this series of numbers. Additionally, each set of numbers determines the potential energy possessed by an electron in that particular level.

Allowed transitions are determined by a series of selection rules. These selection rules can be summed up as the following:

- $\Delta S = 0$
- $\Delta L = \pm 1$

Though other transitions are possible (spin and dipole forbidden respectively), they tend to require an external perturbation in order to induce transition.

Figure shows the what is commonly called a Grotrian diagram for helium. In this diagram, the vertical axis represents the energy above the ground state, and the levels are

arranged horizontally based on increasing L. Levels which are radiatively linked are connected by solid lines. As can be seen in this figure, only the levels having $S = 1$ are radiatively connected to the ground state. As a result, any helium atoms that are excited into the triplet manifold tend to stay there, accumulating in the metastable state, 2^3S.

Approaching 24 eV, the excited electron enters what is known as the continuum. The energy separation between states goes as n^{-2}, thus at large n the spacing becomes quite close and the states are almost indistinguishable. The levels are often referred to as Ryberg states. Above 24.69 eV, the electron becomes totally detached from the helium nucleus, and all that remains is a singly ionized helium atom.

Though the emissions of ions can be quite useful in some plasmas, we do not concern ourselves with them in either the measurements or models. 24.69 eV is the largest known ionization potential, and as a result, the number of ions and the emissions associated with them remain relatively small.

2.2.1 Spectral Lineshapes

It is tempting to think that the energy spacing can be calculated exactly, however there is always some variance about a central energy. This is called the spectral lineshape, and it effects both the energy of the emitted photon in radiative transitions, and the photons that an atom can absorb. Though these variations can be attributed to quantum mechanical effects, the actual result can derived from the so-called dipole approximation.

In this case, we envision a single electron oscillating about a large, heavy, positive charge. The full details of this derivation are covered in Siegman [28], however we'll address some of the most pertinent portions here. The response of a collection of atoms to an applied electric field can be expressed as a quantity known as the susceptibility. This is generally defined as

$$\tilde{\chi}(\omega) \equiv \frac{\tilde{P}(\omega)}{\varepsilon_0 \tilde{E}(\omega)} \tag{2.7}$$

where $\tilde{\chi}$ is the electric susceptibility, $\tilde{P}$ is the macroscopic polarization, $\tilde{E}$ is the applied electric field, and ω is the frequency of the applied field.

Natural Linewidth The electric susceptibility often possesses both a real and imaginary component. Physically, these respectively represent the reactive and absorptive component of the medium. Accounting for level-dependent effects, the standard susceptibility for an

atomic transition can be written as

$$\tilde{\chi}_{\mathrm{at}}(\omega) = -j\frac{3}{4\pi^2}\frac{\Delta N\lambda^3\gamma_{\mathrm{rad}}}{\Delta\omega_{\mathrm{a}}}\frac{1}{1+2j(\omega-\omega_{\mathrm{a}})/\Delta\omega} \tag{2.8}$$

where ΔN represents the population difference between the upper and lower levels of the oscillator, λ is the transition wavelength, γ_{rad} is the natural radiative lifetime of the oscillator, $\Delta\omega_{\mathrm{a}}$ is the linewidth of the transition (for an unperturbed atom, this is simply γ_{rad}), and ω_{a} is the angular frequency of the transition or oscillator.

This equation is generally known as the complex lorentzian. Separated into its components it expresses both the absorptive and reactive properties of the atomic medium. It also clearly susceptible to fields that are displaced from ω_{a}. This is the finite linewidth associated with atomic emissions and absorption.

This linewidth affects each atom within the medium. Each atom will emit or absorb radiation with a probability described by this susceptibility. Consequently, this natural linewidth falls under the homogeneous category of line broadening.

Pressure Broadening Also included in this category is pressure broadening, or more fundamentally, dephasing.

2.2.2 Radiation Trapping

CHAPTER 3

Experiment

3.1 Discharge Apparatus

The discharge apparatus geometry was consistent with the design of a coaxial transmission line. This is similar to the design guidelines provided by Vasilyak [17]. The inner conductor is the plasma generated by the fast ionization wave. Surrounding that is a coaxial dielectric, in this case a quartz tube with 2.75" Conflat flanges on either side. Finally, surrounding the dielectric is the outer conductor or shield. In this case, the shield was an aluminum cylinder with slits of approximately 1.5" by 12" milled lengthwise. Figure **??** is a photograph of this discharge apparatus.

One flange of the quartz tube was held at ground potential, while the other flange was pulsed to approximately 7 kV. Given that the plasma undergoes significant decay between pulses, it is assumed that the impedance is almost infinite when the pulse is first applied, thus the actual voltage on the powered electrode is likely closer to 14 kV. The aluminum shield provides the ground connection for the ground electrode. The two were connected using a copper shim and a compressive shaft collar. The aluminum tube was connected to a second ground shield with a one inch copper braid. This second shield was made of copper and was separated by a teflon cylinder, with walls approximately 1" in thickness, from the powered electrode. Figure **??** is a schematic of the discharge apparatus.

Connected to the powered electrode was a Conflat nipple and an angled quartz window used in the **lcif!** experiments. A short, silicone-coated, high voltage wire connected the window flange to the central conductor of an HN connector. The HN connector was seated on a square copper plate, which was pressed against the shield using four 10-32 screws.

The HN connector was used to attach the transmission line from the high voltage pulser. Initial experiments attempted to use N connectors, however these were susceptible to breakdown in the air gap which separated the center conductor from the outer shield. The transmission line was approximately 15 m in length. Observations, consistent with calculations,

indicated that this provided a window of approximately 140 ns in which to make measurements before the reflected pulse returned to the system and re-energized the plasma.

Attached grounded flange was a second quartz envelope that isolated the ground electrode from the pumping section of the apparatus. Connected to the second quartz envelope was a stainless steel tee, one side of which was connected to an angled quartz window used for the **lcif!** experiments. The other side of the tee was isolated with an alumina break from a series of Conflat fittings connected to a roughing pump. The roughing pump was connected with a shutoff valve, as well as two bypass lines with inline needle valves for flow regulation.

3.2 Measurement Conditions

las!, emission, and coupling energy measurements were made at three different operating pressures. The operating pressures were: 0.3, 0.5, 1.0, 2.0, 3.0, 4.0, 8.0, and 16.0 Torr. Pressures below 10.0 Torr were measured with a capacitance manometer with a full scale range of 10.0 Torr, above this a capacitance manometer with a full scale range of 100.0 Torr was used.

Optical measurements were made at three locations along the axis of the discharge. The measurement location closest to the anode was separated from it by a distance of approximately six inches. Each other optical measurement location was moved further from the anode by an additional three inches.

For each operating condition, measurements were made of the voltage and current. The voltage measurement was made via an internal divider from the power supply. Current measurements were made using an back-current shunt located at a break in the outer shield of the transmission line. The back-current shunt can be seen in Figure **??**. It is composed of nine, low impedance, one ohm resistors, connected in parallel. Each side of the resistors were soldered to a piece of copper foil which was then soldered to the outer shield. A calibrated DC power supply was used to measure the resistance of the current shunt.

All measurements were made using a LeCroy Waverider oscilloscope with a bandwidth of 1 GHz. Connections were made using minimal lengths of RG 50/U cable. When necessary for timing purposes, the cable lengths were matched. Connections were made using minimal lengths of RG 50/U cable. When necessary for timing purposes, the cable lengths were matched. All measurements which required maximum bandwidth were made with a using external 50 ohm terminators.

3.3 Energy Coupling

For comparison to other discharges, estimates of the energy coupling were made using the current and voltage characteristics at each operating pressure.

3.4 Absorption Setup

The **las!** setup was based upon the used of a distributed-feedback laser diode. Temperature and current control of the diode provided coarse and fine tuning, respectively, for the output frequency. It was found that it was unnecessary to adjust the temperature for the diode once the correct transition was found, therefore all tuning was accomplished using current tuning.

The laser diode was produced by Toptica Photonics (model #LD-1083-0070-DFB-1), and had a nominal operating power of 70 mW at a center wavelength of 1083 nm. The diode was held inside a Toptica DL-100 diode housing which contained an integral thermoelectric cooler and collimating optics. The operation of the diode was controlled by a Toptica DC 110 monitor, DCC 110 current control, DTC 110 temperature control, and SC 110 scan control.

A schematic of the optical layout for the absorption experiment can be seen in Figure **??**. Immediately after exiting the housing, the beam was passed through an optical isolator in order to prevent instabilities from back reflections. Next the beam was attenuated using a neutral density filter in order to keep its intensity below the saturation level for the transition. Following that, the beam passed through two apertures for alignment. Here, the beam was split by a partially reflecting mirror. Approximately 98% of the beam was allowed to pass through to a reference photodiode (Thorlabs DET300). After passing through the plasma, entered another aperture to limit near-coincident plasma emissions. The background emissions were further reduced using a long pass filter with a cutoff of 1000 nm. Finally, the beam was coupled into an optical fiber which connected to the detection electronics.

The transmitted laser light was detected with an InGaAs photodiode (Thorlabs DET410). The signal from the diode was often too small to detect, so the output of the signal photodiode was sent through a voltage amplifier (Femto HVA-200M-40-B). The light response of this system is limited by the photodiode which has a nominal rise time of five nanoseconds. The signal from the amplifier was terminated by a 50 ohm terminator and sensed by the aforementioned oscilloscope.

3.4.1 Acquisition Process

The actual acquisition process required a specific series of steps in order to properly account for all noise sources. In order to accommodate this process, a custom LabView script was used to automate the acquisition of the laser transmission spectra. Generally speaking, the signal can be described as

$$V_{\text{total}} = V_{\text{signal}} + V_{\text{background}} + V_{\text{plasma}}. \tag{3.1}$$

In order to remove the background signal, the acquisition scr

3.5 Emissions Setup

CHAPTER 4

Metastable Measurements

CHAPTER 5

Emission Measurements

CHAPTER 6

Modeling

CHAPTER 7

Conclusions

APPENDIX A

Millimeter-Wave Interferometry

$$e = mc^2 \tag{A.1}$$

APPENDIX B

Rotational Spectroscopy

BIBLIOGRAPHY

[1] S M Starikovskaia. Plasma assisted ignition and combustion. *Journal of Physics D: Applied Physics*, 39(16):R265–R299, August 2006.

[2] L B Loeb. Ionizing Waves of Potential Gradient: Luminous pulses in electrical breakdown, with velocities a third that of light, have a common basis. *Science (New York, N.Y.)*, 148(3676):1417–26, June 1965.

[3] L N Kryzhanovsky. Mapping the history of electricity. *Scientometrics*, 17(1-2):165–170, July 1989.

[4] C. Wheatstone. Versuche, die Geschwindigkeit der Elektricität und die Dauer des elektrischen Lichts zu messen. *Annalen der Physik und Chemie*, 110(3):464–480, 1835.

[5] J J Thomson. *Notes on Recent Researches in Electricity and Magnetism*. Clarendon Press, Oxford, UK, 1893.

[6] W. v. Zahn. Spectralröhren mit longitudinaler Durchsicht. *Annalen der Physik und Chemie*, 244(12):675–675, 1879.

[7] J. Beams. The Propagation of Luminosity in Discharge Tubes. *Physical Review*, 36(5):997–1001, September 1930.

[8] C V Boys. Progressive Lightning. *Nature*, 118(2977):749–750, November 1926.

[9] B. F. J. Schonland, D. J. Malan, and H. Collens. Progressive Lightning. II. *Proceedings of the Royal Society A: Mathematical, Physical and Engineering Sciences*, 152(877):595–625, November 1935.

[10] T E Allibone and J M Meek. The Development of the Spark Discharge. *Proceedings of the Royal Society A: Mathematical, Physical and Engineering Sciences*, 166(924):97–126, May 1938.

[11] E. Flegler and H. Raether. Der elektrische Durchschlag in Gasen nach Untersuchungen mit der Nebelkammer. *Zeitschrift f r Physik*, 99(9-10):635–642, September 1936.

[12] Leonard B. Loeb and John M. Meek. The Mechanism of Spark Discharge in Air at Atmospheric Pressure. I. *Journal of Applied Physics*, 11(6):438, June 1940.

[13] L. Fisher and B. Bedderson. Formative Time Lags of Spark Breakdown in Air in Uniform Fields at Low Overvoltages. *Physical Review*, 81(1):109–114, January 1951.

[14] R. G. Fowler and B. D. Fried. Theory of Electron Driven Shock Waves. *Physics of Fluids*, 4(6):767, 1961.

[15] Gennadii A Mesyats, Yu I Bychkov, and V V Kremnev. Pulsed nanosecond electric discharges in gases. *Soviet Physics Uspekhi*, 15(3):282–297, March 1972.

[16] E Kunhardt and W Byszewski. Development of overvoltage breakdown at high gas pressure. *Physical Review A*, 21(6):2069–2077, June 1980.

[17] L M Vasilyak, S V Kostyuchenko, N N Kudryavtsev, and I V Filyugin. Fast ionisation waves under electrical breakdown conditions. *Physics-Uspekhi*, 37(3):247–268, March 1994.

[18] N B Anikin, S V Pancheshnyi, S M Starikovskaia, and A Yu Starikovskii. Breakdown development at high overvoltage: electric field, electronic level excitation and electron density. *Journal of Physics D: Applied Physics*, 31(7):826–833, April 1998.

[19] S M Starikovskaia, N B Anikin, S V Pancheshnyi, D V Zatsepin, and A Yu Starikovskii. Pulsed breakdown at high overvoltage: development, propagation and energy branching. *Plasma Sources Science and Technology*, 10(2):344–355, May 2001.

[20] S.V. Pancheshnyi, S.M. Starikovskaia, and A.Yu. Starikovskii. Measurements of rate constants of the v =0) and v =0) deactivation by N2, O2, H2, CO and H2O molecules in afterglow of the nanosecond discharge. *Chemical Physics Letters*, 294(6):523–527, September 1998.

[21] S V Pancheshnyi, S M Starikovskaia, and A Yu Starikovskii. Population of nitrogen molecule electron states and structure of the fast ionization wave. *Journal of Physics D: Applied Physics*, 32(17):2219–2227, September 1999.

[22] S.O. Macheret, M.N. Shneider, and R.B. Miles. Modeling of air plasma generation by repetitive high-voltage nanosecond pulses. *IEEE Transactions on Plasma Science*, 30(3):1301–1314, June 2002.

[23] Igor V Adamovich, Munetake Nishihara, Inchul Choi, Mruthunjaya Uddi, and Walter R Lempert. Energy coupling to the plasma in repetitive nanosecond pulse discharges. *Physics of Plasmas*, 16(11):113505, 2009.

[24] Dmitry S. Nikandrov, Lev D. Tsendin, Vladimir I. Kolobov, and Robert R. Arslanbekov. Theory of Pulsed Breakdown of Dense Gases and Optimization of the Voltage Waveform. *IEEE Transactions on Plasma Science*, 36(1):131–139, 2008.

[25] L D Tsendin and D S Nikandrov. An analytical approach to planar ionization fronts in dense gases. *Plasma Sources Science and Technology*, 18(3):035007, August 2009.

[26] Yvette Zuzeek, Inchul Choi, Mruthunjaya Uddi, Igor V Adamovich, and Walter R Lempert. Pure rotational CARS thermometry studies of low-temperature oxidation kinetics in air and ethene–air nanosecond pulse discharge plasmas. *Journal of Physics D: Applied Physics*, 43(12):124001, March 2010.

[27] Michael A. Lieberman and Allan J. Lichtenberg. *Principles of Plasma Discharges and Materials Processing*. John Wiley & Sons, Inc., Hoboken, NJ, USA, 2nd edition, April 2005.

[28] A. E. Siegman. *Lasers*. University Science Books, Sausalito, CA, 1986.